Modelling and analysis of planar cell polarity

S. Schamberg, P. Houston, N. A. M. Monk, M. R. Owen

November 10, 2008

Abstract

Planar cell polarity (PCP) occurs in the epithelia of many animals and can lead to the alignment of hairs, bristles and feathers; physiologically, it can organise ciliary beating. Here we present two approaches to modelling this phenomenon. The aim is to discover the basic mechanisms that drive PCP, while keeping the models mathematically tractable. We present a feedback and diffusion model, in which adjacent cell sides of neighbouring cells are coupled by a negative feedback loop and diffusion acts within the cell. This approach can give rise to polarity, but also to period two patterns. Polarisation arises via an instability provided a sufficiently strong feedback and sufficiently weak diffusion. Moreover, we discuss a conservative model in which proteins within a cell are redistributed depending on the amount of proteins in the neighbouring cells, coupled with intracellular diffusion. In this case polarity can arise from weakly polarised initial conditions or via a wave provided the diffusion is weak enough. Both models can overcome small anomalies in the initial conditions. Furthermore, the range of the effects of groups of cells with different properties than the surrounding cells depends on the strength of the initial global cue and the intracellular diffusion.

1 Introduction

During development, polarity is a common feature of many cell types. One example is the polarisation of whole fields of epithelial cells within the plane of the epithelium, a phenomenon called planar cell polarity (PCP). It is widespread in nature and plays important roles in development and physiology. Prominent examples include the epithelial cells of the wing, leg, abdomen and eye of insects like the fruit fly *Drosophila melanogaster* [1], polarised tissue morphogenesis in vertebrates and sensory hair cells in vertebrate ear (reviewed in [13]). The underlying dynamics are not fully understood yet, but it is general consensus that PCP is driven by a three-tiered mechanism. The first tier provides directional cues to each cell, the second amplifies these cues via a feedback loop and the third tier performs the readout. Tiers one and three seem to be tissue specific, whereas a network of proteins centred around the transmembrane protein Frizzled, also referred to as core proteins, may constitute a mechanism for tier two that is common to all tissues.

In many cases PCP signalling organises the polarity of cells in a coordinated fashion over a whole tissue, as manifested in the alignment of structures such as bristles, hairs or feathers. For example, in the *Drosophila* wings every cell elaborates a hair that points distally. Experimentally induced clonal clusters of cells in which the function of the core network components is disrupted (e.g. by mutation or

mis-expression) induce domineering nonautonomy, characterised by hairs in the surrounding wild-type cells pointing in wrong directions [16]. This striking phenomenon shows that polarity is disrupted not only in cells of the clone, but also in neighbouring cells, and suggests that intercellular signalling contributes to amplifying polarity in tier two.

Two models for PCP, focusing on the wing of the fruit fly, have been developed by Amonlirdviman *et al.* ([2], [12]) and Le Garrec *et al.* [8] (applied to the *Drosophila* eye in [7]). Both models centre around the idea of amplification of polarity via asymmetric complex formation of the core proteins. This is based on experimental results, which show that in the wing the core proteins become distributed asymmetrically along the proximal-distal axis just before the initiation of hair growth [14]. Both models are encoded as large systems of differential equations and solved numerically in two dimensions for hexagonal shaped cells. Therefore, they tend to be rather complex and do not lend themselves to mathematical analysis very easily. Furthermore, because of the lack of appropriate biological data, the feedback mechanisms in these models are mainly based on assumptions.

Our aim is to assess the nature of PCP in a more generic setting that encompasses a broad class of specific models. To this end, we have developed two models for the generation of planar cell polarity based on juxtacrine signalling. This is supported by the findings of Chen *et al.* [3] that one of the core proteins, Flamingo, forms homodimers between neighbouring cells and functions as a signal to mediate intercellular signalling of two other core components, Frizzled and Van Gogh [17].

Our first model is the feedback and diffusion model in which a positive feedback loop couples adjacent cell sides of neighbouring cells and diffusion acts within a cell. It is a non-conservative approach because regulated production and degradation of proteins are included. In section 2 we carry out analysis and numerical simulations for this model.

Our second approach is based on a conservative model, in which the proteins in each cell are just redistributed. We assume that this redistribution within a cell depends on its neighbouring cells; this is also coupled with intracellular diffusion. The analysis and numerical simulations for this model are presented in section 3.

These generic approaches give us the opportunity to get some insight into the basic mechanisms present in PCP. Our main targets are to investigate the dependence of PCP emergence on the strength of the feedback and the strength of the diffusion; analyse their potential to overcome anomalies in the initial conditions; and investigate the behaviour of the system for clones – groups of cells that have a different amount of proteins or a different strength of feedback than the rest of the cells.

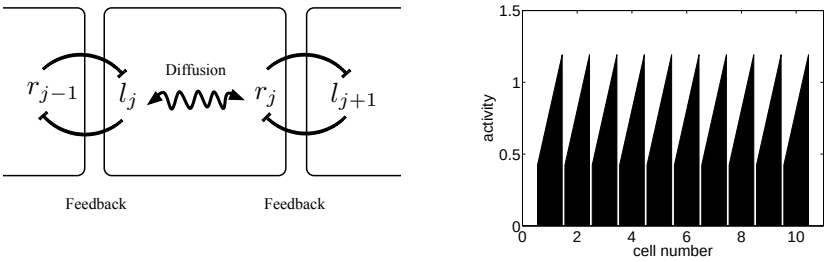

(a) (b)

Figure 1: Illustration of the Feedback and Diffusion Model; (a) shows the mechanism of the feedback and diffusion model and (b) an example of a homogeneous polarised steady state.

2 Feedback and Diffusion Model

We consider first a one-dimensional line of cells each having two sides, with r_j and l_j representing generic PCP activities on the right and left side of cell j, respectively. These activities can be regarded as accumulations of certain PCP proteins. We assume that adjacent faces of neighbouring cells inhibit each other by juxtacrine intercellular signalling and that these interactions are described by the following system of equations:

$$\begin{aligned} \dot{l}_j &= -l_j + f(r_{j-1}) + d(r_j - l_j), \\ \dot{r}_j &= -r_j + f(l_{j+1}) + d(l_j - r_j), \end{aligned} \tag{1}$$

where f is a decreasing positive function representing inhibition, with $f(0)$ finite and positive. In the examples that follow, we choose $f(x) = ce^{-x^2}$ or $f(x) = \frac{1}{1+qx^k}$ with positive c, q and k, where the first choice is a one-parameter family and the second one a two-parameter family of inhibition functions. The coefficient $d \geq 0$ in (1) measures the rate of intracellular diffusion of PCP activity. This is summarised in Figure 1(a).

We have a system in which the feedback loop gives a pattern forming potential such that at the interface between cells we have low activity on one cell side next to high activity in the adjacent side of the neighbouring cell; diffusion couples this within a cell to give coherence. Our objective is to investigate this interplay quantitatively.

We refer to the case when all cells are the same at steady state, i.e., $l_j = L$ and $r_j = R$ for all j, as a homogeneous steady state of the system (1). If $L = R$ we call it a homogeneous unpolarised steady state and if $L \neq R$ a homogeneous polarised steady state. Figure 1(b) shows an example of a homogeneous polarised steady state.

For the subsequent analysis we assume that we have an infinite row of cells.

2.1 Existence of steady states

System (1) always has a unique homogeneous unpolarised steady state U with $U = l_j = r_j$, because in this case the corresponding steady state equations reduce to $U = f(U)$ which has a unique solution since f is decreasing. Assuming a homogeneous steady state (L, R) exists, (1) reduces to a system of two ODEs, with nullclines given by

$$L = \frac{f(R) + dR}{1 + d}, \quad R = \frac{f(L) + dL}{1 + d}.$$

Setting $g(x) := \frac{f(x)+dx}{1+d}$, we see that $g(0)$ is finite and positive. Furthermore, $\lim_{x\to\infty} g(x) \geq 0$. The system has a pair of homogeneous polarised steady states if $g'(U) < -1$, i.e., $\frac{f'(U)+d}{1+d} < -1$. This implies $d < -\frac{f'(U)+1}{2}$. Since $d \geq 0$, this leads to the condition $f'(U) < -1$, which is necessary but not sufficient. At a homogeneous polarised steady state (L, R) the inequality $\left(\frac{f'(R)+d}{1+d}\right)\left(\frac{f'(L)+d}{1+d}\right) < 1$ holds. Examples of L- and R-nullclines of systems with homogeneous polarised steady states are shown in Figure 2.

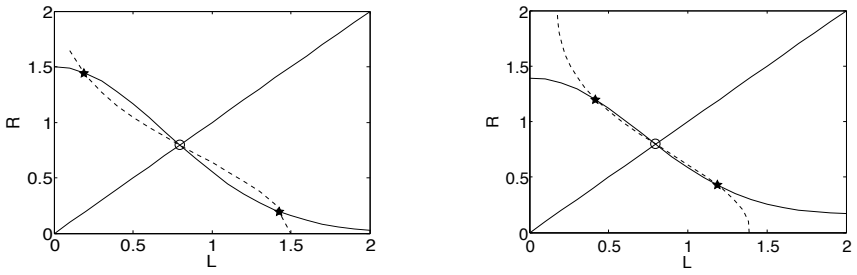

(a) (b)

Figure 2: Nullclines for homogeneous states of (1) with $f(x) = 1.5e^{-x^2}$ and different choices of d; (a) $d = 0$; (b) $d = 0.08$. The solid lines are the R-nullclines and the dashed lines the L-nullclines, the homogeneous polarised steady states are indicated by stars, and the homogeneous unpolarised steady state by a circle.

We next investigate the existence of an unpolarised period two pattern, i.e., $l_j = r_j = V$ red for j even and $l_j = r_j = W$ for j odd. Since this pattern is independent of diffusion, system (1) reduces to

$$\dot{W} = -W + f(V),$$
$$\dot{V} = -V + f(W),$$

which is essentially the same as the lateral inhibition system analysed in [4]. The period two pattern exists if $f'(U) < -1$ at the homogeneous steady state U of (1).

2.2 Stability analysis

In this section we analyse the stability of the homogeneous steady states of system (1) to homogeneous and inhomogeneous perturbations. We start by linearising the system about a homogeneous steady

state (L, R). Thus, with $l_j = L + \widetilde{l}_j$ and $r_j = R + \widetilde{r}_j$, neglecting terms higher than first order, we get

$$\begin{aligned}\dot{\widetilde{l}}_j &= -\widetilde{l}_j + f'(R)\widetilde{r}_{j-1} + d(\widetilde{r}_j - \widetilde{l}_j),\\ \dot{\widetilde{r}}_j &= -\widetilde{r}_j + f'(L)\widetilde{l}_{j+1} + d(\widetilde{l}_j - \widetilde{r}_j).\end{aligned}$$

Suppose the solutions of the above system are of the form $\widetilde{l}_j = L_0 e^{ikj+\lambda t}$ and $\widetilde{r}_j = R_0 e^{ikj+\lambda t}$, respectively, where λ is the growth rate of perturbations with wave number k. Substituting into the linearised equations, dividing by $e^{ikj+\lambda t}$ and omitting the tildes yields

$$\begin{aligned}\lambda L_0 &= -L_0 + f'(R)R_0 e^{-ik} + d(R_0 - L_0),\\ \lambda R_0 &= -R_0 + f'(L)L_0 e^{ik} + d(L_0 - R_0).\end{aligned} \tag{2}$$

Nontrivial solutions of system (2) require

$$0 = \det\left[\begin{pmatrix} -1-d & f'(R)e^{-ik}+d \\ f'(L)e^{ik}+d & -1-d \end{pmatrix} - \lambda I\right] = \det(A - \lambda I). \tag{3}$$

If $\mathrm{Re}\lambda < 0$ for both solutions of (3), the homogeneous steady state is stable. Equivalently, for stability $\mathrm{tr}(A) < 0$ and $\det(A) > 0$ have to hold. The first condition ($\mathrm{tr}(A) < 0$) is always fulfilled. To investigate the second one, we consider the case where the homogeneous steady state is both stable to homogeneous perturbations (i.e., for $k = 0$) and unstable to inhomogeneous perturbations (i.e., for at least one $k \neq 0$).

Homogeneous unpolarised steady state

First we suppose $L = R = U$, i.e., we consider a homogeneous unpolarised steady state. Furthermore, assume $k = 0$, i.e., a homogeneous perturbation. Then, we get $\det(A) = 1 + 2d(1 - f'(U)) - f'(U)^2$, which is greater than 0 if $d > -\frac{f'(U)+1}{2}$ since $f'(U) < 0$.

Now consider $k \neq 0$. For the determinant we get $\det(A) = 1 + 2(1 - f'(U)\cos k)d - f'(U)^2$. If $d = 0$ the homogeneous steady state is unstable for all $k \neq 0$ if $f'(U) < -1$. Otherwise, it is unstable if

$$\cos k < -\frac{f'(U)^2 - 1 - 2d}{2df'(U)}, \quad \text{for some } k \neq 0.$$

Hence, d has to satisfy

$$-1 < -\frac{f'(U)^2 - 1 - 2d}{2df'(U)}.$$

Since $f'(U) < 0$ and $d > 0$ we get

$$2d(f'(U) + 1) < f'(U)^2 - 1 = (f'(U) + 1)(f'(U) - 1).$$

Thus,

$$2d < f'(U) - 1, \text{ if } f'(U) > -1 \tag{4}$$

and

$$2d > f'(U) - 1, \text{ if } f'(U) < -1. \tag{5}$$

We see that equation (4) implies $d < 0$, which contradicts our assumptions, whereas (5) holds for all d. Hence, for $f'(U) < -1$ the homogeneous unpolarised steady state is unstable to inhomogeneous perturbations.

Combining the results for $k = 0$ and $k \neq 0$ we conclude that if $f'(U) < -1$ and $d > -\frac{f'(U)+1}{2}$ hold, system (1) exhibits spatial instabilities. Since Reλ is maximal if det(A) is minimal and $k = \pi$ is a minimum of det(A), π is the fastest growing mode. Hence, we expect to observe patterns of period two.

To clarify these results Figure 3 shows the dispersion relation $\lambda(k)$ of the largest eigenvalue λ of system (1) for the inhibition function $f(x) = 1.5e^{-x^2}$ and different values of d. In this case $f'(U) = -1.1682$ for the homogeneous unpolarised steady state U and therefore both the figure and the analysis above show that there are instabilities for all $d > 0.0841$.

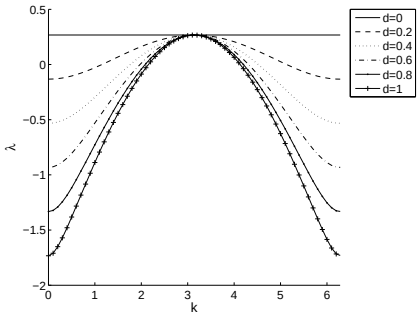

Figure 3: Dispersion relation for the homogeneous unpolarised steady state ($f(x) = 1.5e^{-x^2}$, different values of d); $d = 0$, the homogeneous unpolarised steady state is unstable to homogeneous perturbations, the polarised steady state arises; $d \geq 0.2$, the homogeneous unpolarised steady state is stable to homogeneous perturbations and unstable to inhomogeneous perturbations, we get period two patterns.

Homogeneous polarised steady state

As a next step we investigate the case $L \neq R$. The corresponding matrix is

$$A = \begin{pmatrix} -1-d & f'(R)e^{-ik}+d \\ f'(L)e^{ik}+d & -1-d \end{pmatrix}$$

and its determinant is given by

$$\det(A) = 1 + 2d - f'(L)f'(R) - (f'(L)e^{ik} + f'(R)e^{-ik})d.$$

For $k = 0$ we wish to obtain stability. Hence, we get $d > \frac{f'(L)f'(R)-1}{2-(f'(L)+f'(R))}$ which is true for all $d \geq 0$, because f is decreasing and $f'(L)f'(R) < 1$ (see Section 2.1). Again we seek instability for at least

one $k \neq 0$. Therefore, we get $d < \frac{f'(L)f'(R)-1}{2-(f'(L)e^{ik}+f'(R)e^{-ik})} < 0$. This is a contradiction since we chose $d \geq 0$. Thus, if homogeneous polarised steady states exist they are always stable.

Period two patterns

We continue by analysing the stability of period two patterns. We take every two cells together and label their sides with l_j, mr_j, ml_j, and r_j (derived from "left", "middle right", "middle left" and "right" side, respectively). We linearise about a steady state (V, W) using $l_j = V + \widetilde{l_j}, mr_j = V + \widetilde{mr_j}, ml_j = W + \widetilde{ml_j}$ and $r_j = W + \widetilde{r_j}$. Omitting higher order terms, this yields

$$\begin{aligned}
\dot{\widetilde{l_j}} &= -\widetilde{l_j} + f'(W)\widetilde{r_{j-1}} + d(\widetilde{mr_j} - \widetilde{l_j}),\\
\dot{\widetilde{mr_j}} &= -\widetilde{mr_j} + f'(W)\widetilde{ml_j} + d(\widetilde{l_j} - \widetilde{mr_j}),\\
\dot{\widetilde{ml_j}} &= -\widetilde{ml_j} + f'(V)\widetilde{mr_j} + d(\widetilde{r_j} - \widetilde{ml_j}),\\
\dot{\widetilde{r_j}} &= -\widetilde{r_j} + f'(V)\widetilde{l_{j+1}} + d(\widetilde{ml_j} - \widetilde{r_j}).
\end{aligned}$$

Now suppose $\widetilde{l_j} = Ae^{ikj+\lambda t}, \widetilde{mr_j} = Be^{ikj+\lambda t}, \widetilde{ml_j} = Ce^{ikj+\lambda t}$ and $\widetilde{r_j} = De^{ikj+\lambda t}$. Therefore, we get

$$\begin{aligned}
\lambda A &= -A + f'(V)De^{-ik} + d(B - A),\\
\lambda B &= -B + f'(V)C + d(A - B),\\
\lambda C &= -C + f'(W)B + d(D - C),\\
\lambda D &= -D + f'(W)Ae^{ik} + d(C - D),
\end{aligned}$$

and the corresponding matrix is

$$\begin{pmatrix}
-1-d & d & 0 & f'(V)e^{-ik}\\
d & -1-d & f'(V) & 0\\
0 & f'(W) & -1-d & d\\
f'(W)e^{ik} & 0 & d & -1-d
\end{pmatrix}.$$

Let $k = 0$, i.e., assume period two pattern. The eigenvalues in this case are

$$\begin{aligned}
\lambda_1 &= -1 + \sqrt{f'(V)f'(W)},\\
\lambda_2 &= -1 - \sqrt{f'(V)f'(W)},\\
\lambda_3 &= -2d - 1 + \sqrt{f'(V)f'(W)},\\
\lambda_4 &= -2d - 1 - \sqrt{f'(V)f'(W)}.
\end{aligned}$$

Whenever the period two pattern exists $f'(W)f'(V) < 1$ holds, and therefore $\mathrm{Re}\lambda_i < 0$ for all $i = 1, ..., 4$. Hence, this state is always stable to perturbations of period two or less.

Now consider $k \neq 0$. The eigenvalues in this case are too complex to study analytically, but numerical

analysis suggests that this steady state is always stable to inhomogeneous perturbations. Figure 4 shows the dispersion relation of the largest eigenvalue for a particular choice of f and different d. As we can see the steady state is stable for every $d > 0$ we have chosen, which supports the results of the numerical analysis.

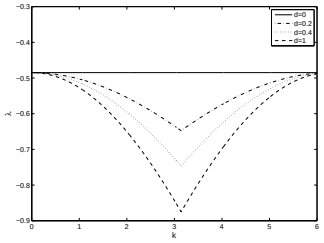

Figure 4: Dispersion relation for the growth rate of period two spatial perturbations ($f(x) = 1.5e^{-x^2}$, different values of d); the period two pattern is always stable.

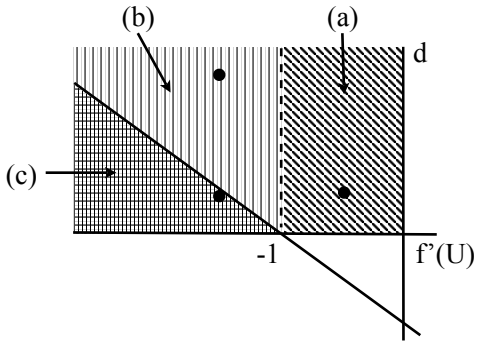

(a) Homogeneous unpolarised steady state is stable: both cell sides are equal

(b) Period two patterns are stable

(c) Period two patterns are stable; homogeneous polarised steady states are stable: polarisation

Figure 5: Summary of the dependence of the stability of steady states on $f'(U)$ and d. The dots indicate the parameter values chosen for the simulations in Figure 6 (see Section 2.3).

The results of our linear stability analysis are summarised in Figure 5. There are three regions of interest. Region (a) is characterised by $0 > f'(U) > -1$. For values in this region, the homgeneous unpolarised steady state of system (1) is stable. Regions (b) and (c) are seperated by the line $d = -\frac{f'(U)+1}{2}$ (see Section 2.1). The period two pattern is stable in region (b) as well as region (c). The homegeneous polarised steady state is only stable in region (c).

2.3 Numerical simulations

System (1) was simulated for a row of 100 cells, using the Matlab ODE solver ode45. At the boundaries we assumed $r_0 = r_1$ and $l_{101} = l_{100}$. Periodic boundary conditions gave similar results (results not shown). Both are compatible with the boundary condition chosen for the analysis of the homogeneous

steady states, but are incompatible with our analysis of the period two patterns. However, in this case the effects of the boundary conditions are restricted to the three cells closest to the boundaries as can be seen in Figure 6.

The plots in Figures 6–9 were generated using $f(x) = ce^{-x^2}$ with different values for c, different values for d and four different types of initial conditions. We have also considered $f(x) = \frac{1}{1+qx^k}$ with positive q and k, but the results were similar, as expected from the analysis. For clarity, only the first 10 cells are shown in each figure, but the patterns continue in the obvious way.

In the second column of Figure 6 we see that all cells evolve to the homogeneous unpolarised steady state irrespective of the initial conditions, if $c = 0.5$ and $d = 0.1$. These results stay the same if d is increased. This is consistent with our analysis, because for this choice of parameters $f'(U) > -1$ at the homogeneous unpolarised steady state U and therefore we are in region (a) of Figure 5. Hence, by increasing d we do not cross any bifurcation lines.

The figures in the third column of Figure 6 display the final state for $d = 0.4$ and $c = 1.5$, with different initial conditions shown in the first column of Figure 6. For these simulations we are in region (b) of Figure 5. Hence, the numerical results support the results from the analysis that the unpolarised steady state is stable to homogeneous perturbations. For inhomogeneous perturbations, period two patterns arise, spreading out as a wave. Similar waves have been investigated in [11]. As expected, the same patterns result if d is increased.

The results in the last column of Figure 6 show the final states for $c = 1.5$ and $d = 0.08$ and the three different initial conditions displayed in the first column of Figure 6, respectively. They do not change if d is decreased which again can be explained by looking at Figure 5 since we are now in region (c). The last column of Figure 6 illustrates the fact that the homogeneous polarised steady state and the inhomogeneous period two pattern are both stable for the same parameter values. The final state achieved depends on the initial condition. Because of this we had a closer look at the initial conditions by moving gradually from the one in the second row of Figure 6 to the one in the third row. Therefore we decreased the initial value $r_j(0)$ for $j \geq 2$ from 1.1 to 0.5 in 0.1 steps while $l_j(0) = 0.5$ for $j \geq 2$. The results are that down to $r_j(0) = 0.9$ the cells become stably polarised. For $r_j(0) = 0.8$ to $r_j(0) = 0.6$ the cells are polarised transiently, but subsequently a patterning wave arises from the left end of the row for the boundary conditions $r_0 = r_1$ and $l_{101} = l_{100}$ or from both ends for periodic boundary conditions. If $r_j(0) = 0.5$ the patterning wave starts immediately and no polarisation takes place. However, if we weaken the initial polarity of the initial condition in the second row of Figure 6 and decrease d we can still get the homogeneous polarised steady state.

These results show that apart from a small d and small $f'(U)$ we also need sufficiently uniform initial

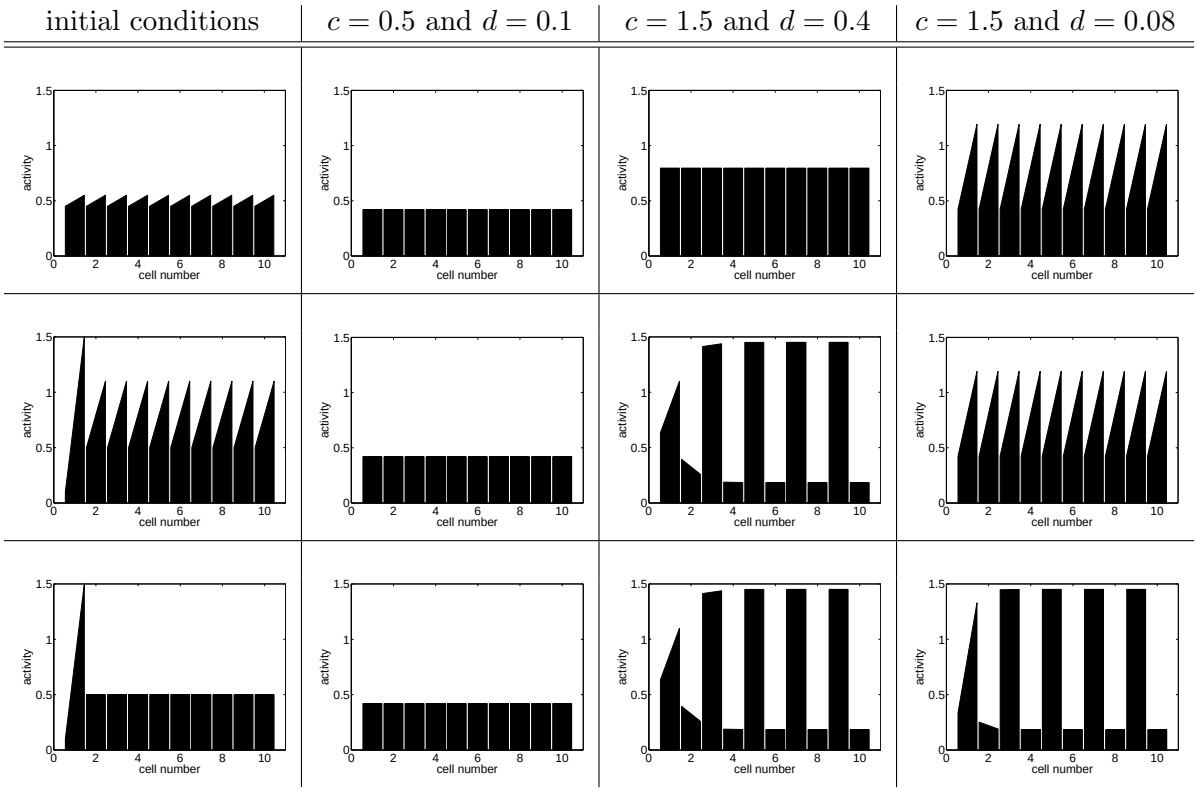

Figure 6: Steady state patterns of PCP activity for system (1) for different initial conditions and different choices of c and d. 100 cells were simulated, but only the first 10 are shown, for clarity. Patterns in the rest of the domain continue in the obvious way.

conditions to achieve polarity. Inhomogeneous initial conditions will give rise to period two patterns, which always spread as a wave. Therefore, a small diffusion coefficient d is essential to overcome anomalies in initial conditions. This dependence is shown in Figure 7. If d is small enough the model can overcome random noise in the system as well as correct single cells that are initially polarised in the opposite direction to the surrounding cells (see Figure 7(b)). However, these single cells have to be more weakly polarised than their neighbours. If we increase d the cells pointing in the opposite direction give rise to a period two pattern (shown in Figure 7(c)).

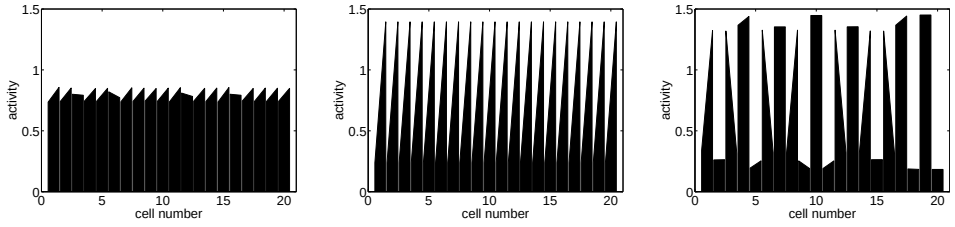

(a) (b) (c)

Figure 7: Initial condition with errors and the corresponding final states for system (1) for different values of d and c; (a) initial condition, (b) result for $d = 0.02$ and $c = 1.5$, (c) result for $d = 0.08$ and $c = 1.5$.

Analysis of clones

To study PCP experimentally, clonal clusters of cells in which a certain gene is either knocked out or overexpressed, are induced in the tissue [18]. The behaviour of the wild-type tissue around the clone gives insight into the interplay of the genes involved in the process.

We consider two different ways of representing clones in our model. In the first, we change the initial amount of activity in a group of cells in the row while having the same feedback in all cells. In the second, we alter the strength of the feedback in a group of cells while having the same initial amount of activity in every cell. The results of the first method (inclusion of a few cells in the row that have less activity than the rest) are shown in Figure 8.

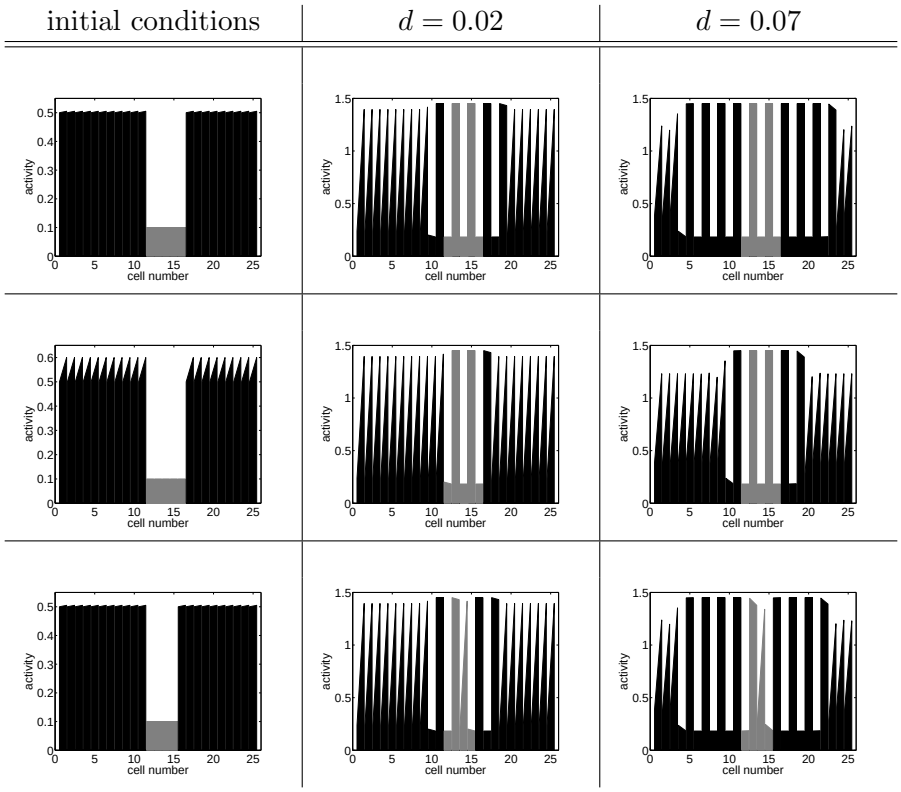

Figure 8: First column: initial conditions for clones containing either an odd or even number of cells that have less initial activity in each cell than the surrounding cells and different strength of initial global cue in the wild-type cells. The difference between left and right side in the first and third row is 0.05 and in the second row 0.1; second and third column: the corresponding final states for system (1) for $c = 1.5$ and different diffusion parameters.

We have considered clones comprising either an odd or even number of cells. Initially, we have chosen two different strengths of global cue in the cells surrounding the clone. The difference between left and right in the wild-type cells in the initial conditions in the first and third row of Figure 8 is 0.05 and in the second row 0.1. The second and third column of Figure 8 correspond to different values for the diffusion parameter. In all cases we observe a wave of period two pattern, which is initiated at

the interface between the clone and the surrounding cells and moves in both directions. How far this wave spreads depends on the strength of the initial cue in the surrounding cells and the diffusion. For a strong initial cue and small diffusion we get a short range of the effect of the clone. Increasing the diffusion or decreasing the strength of the initial global cue in the wild-type cells increases the range of the effect of the clone as shown in the first two rows of Figure 8.

For the even numbered clone we get similar results, apart from a peak that occurs in the clone instead of a regular period two pattern. The results for a weak initial global cue in the cells surrounding the clone are shown in the third row of Figure 8. Results for a strong initial global cue are analogous (not shown). We get similar results if the activity in the cells in the clone is higher than in the rest of the cells (results not shown).

Figure 9 shows the result of changing the strength of the feedback in a group of cells. The clones in the first and second rows of Figure 9 have an odd and even number of cells, respectively. In the initial conditions we chose the weak global cue with a difference of 0.05 between left and right sides in the cells surrounding the clone. The diffusion parameter is set to 0.02. The second and third column of Figure 9 differ in the choice of feedback strength in the clone. In the second column we chose $c = 1.4$ and in the third $c = 0.5$. The feedback in the surrounding cells is always set to $c = 1.5$. The two choices of feedback strength for the clone cells represent two different cases of steady state behaviour. For $c = 1.4$ the homogeneous unpolarised steady state is unstable and period two patterns or polarisation can arise; for $c = 0.5$ the homogeneous unpolarised steady state is stable.

In the first row of Figure 9 we see that the period two patterning wave which is initiated at the edges of the clone spreads in both directions for $c = 1.4$, but does not pattern the clone for $c = 0.5$. In this case the cells in the clone are unpolarised. The second row of Figure 9 shows that going from odd numbers of cells in the clone to even numbers only the result for $c = 1.4$ changes essentially. Here, again we see the peak arising in the clone, because the number of cells in the clone is not compatible with the period of the pattern. Increasing the feedback strength above $c = 1.5$ yields similar results to those for $c = 1.4$. We omit the results for changing the diffusion parameter and the strength of the initial global cue in the wild-type cells, but they give the same dependence as shown in Figure 8 for the clone with a different amount of activity than in the surrounding cells.

In all cases a wave of period two pattern is initiated at the clone boundaries and spreads out into the surrounding cells with the range depending on the parameter values. The cells within the range of the effect of the clone thus do not have an intracellular difference of activity, i.e., no polarity. This is different to the phenomenon of domineering nonautonomy, which is seen in experiments. Depending on which protein is lacking in the clone, polarity can be disrupted in such a way that the hairs in a

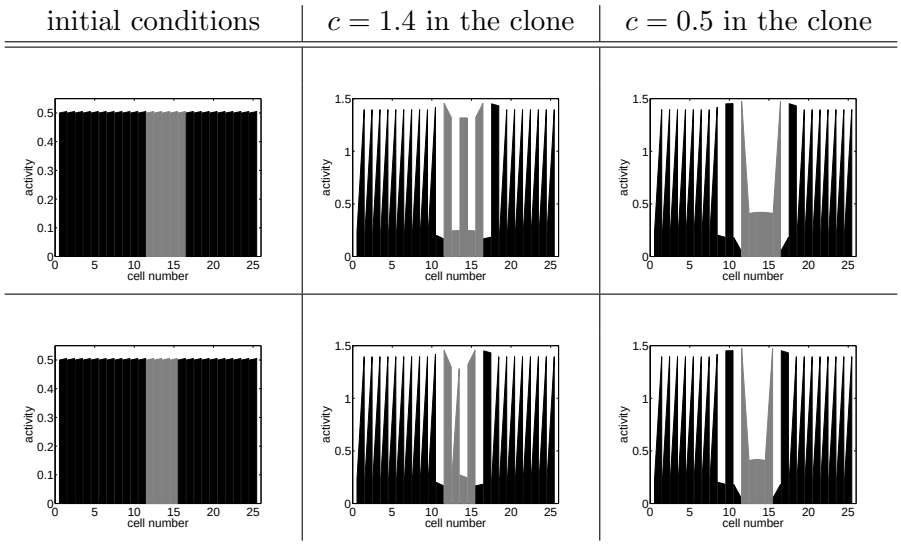

Figure 9: First column: initial conditions with odd and even numbered clones with different feedback strength, surrounded by cells with feedback $c = 1.5$. All cells have a weak initial bias – the difference between left and right is 0.05. Second and third columns: corresponding final states for system (1) for $c = 1.4$ and $c = 0.5$ in the clone and $d = 0.02$.

few cells behind the clone point in the opposite direction to the rest of the wild-type cells. Therefore, the experimental results show that the cells within the range of the effect of the clone have a polarity.

3 Conservative model

The second approach we consider is based on employing a conservative model. It describes the dynamic redistribution of conserved PCP activities within the membrane of each cell. We again consider a row

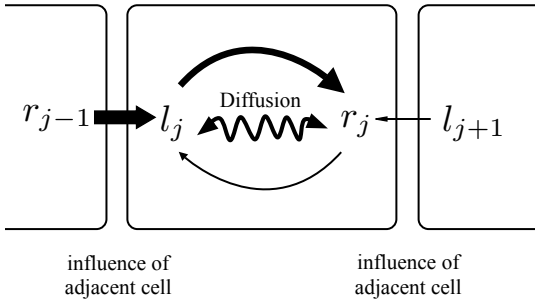

Figure 10: Schematic representation of the mechanism of the conservative model. A conserved PCP activity within each cell is redistributed in response to juxtacrine intercellular signalling and intracellular diffusion.

of two-sided cells with r_j representing a generic PCP activity on the right side and l_j on the left side of cell j. These values may represent amounts of certain proteins. Additionally, the total amount of activity in each cell is conserved, thus $l_j + r_j = Q$ for all j. In contrast to the feedback and diffusion

model, the amount of activity in a cell is not raised and lowered but redistributed within the cell, depending on the amount of activity in the adjacent sides of the neighbouring cell. The model is encoded by the following equations

$$\begin{aligned} \dot{l_j} &= g(l_{j+1})r_j - g(r_{j-1})l_j + d(r_j - l_j), \\ \dot{r_j} &= g(r_{j-1})l_j - g(l_{j+1})r_j + d(l_j - r_j), \end{aligned} \tag{6}$$

where g is an increasing positive function, representing the influence of the adjacent cells on the movement, and $d \geq 0$ denotes the diffusion. Hence, if we look at a cell side and there is a large amount of activity in the adjacent side of the neighbouring cell then a large proportion of the PCP activity on the present cell side gets moved away from it. Similarly, if there is only a small amount of activity in the adjacent side of the neighbouring cell only a small proportion of the amount on the current side gets moved. Therefore cell sides with large amounts of activity in them repel activity in the adjacent side of the neighbouring cell and small amounts attract activity to the adjacent side in the neighbouring cell. The amount of activity at a cell side depends on the adjacent cell sides of both neighbours, because they determine how much gets moved toward this cell side and how much gets moved away from it.

We again apply a steady state analysis followed by numerical simulations. For the steady state analysis we assume an infinite row of cells.

3.1 Existence of steady states

Substitution of $r_j = Q - l_j$ into (6) and setting $L_j := \frac{l_j}{Q}$ yields

$$\dot{L_j} = g(L_{j+1})(1 - L_j) - g(1 - L_{j-1})L_j + d(1 - 2L_j). \tag{7}$$

Our rescaling implies $0 \leq L_j \leq 1$. The homogeneous unpolarised steady state is $L_j = \frac{1}{2}$ for all j, which always exists. A homogeneous polarised steady state $L \neq \frac{1}{2}$ exists if

$$d = \frac{g(1-L)L - g(L)(1-L)}{1-2L}. \tag{8}$$

Defining $d(L) := \frac{g(1-L)L - g(L)(1-L)}{1-2L}$, this function has a singularity at $L = \frac{1}{2}$. Furthermore, we get $d(0) = d(1) = -g(0)$. Since g is a positive function and d has to be nonnegative the completely polarised homogeneous steady states $L = 1$ or $L = 0$ exist only if $g(0) = 0$.

Following the same arguments, reformulating (8) yields that a steady state L with $0 < L < \frac{1}{2}$ exists only if

$$\frac{g(1-L)}{g(L)} > \frac{1-L}{L} \quad \text{for} \quad 0 < L < \frac{1}{2} \tag{9}$$

and a steady state with $\frac{1}{2} < L < 1$ only if

$$\frac{g(1-L)}{g(L)} < \frac{1-L}{L} \quad \text{for} \quad \frac{1}{2} < L < 1. \tag{10}$$

Figures 11 and 12 show plots for $g(L)$, $\frac{g(1-L)}{g(L)}$, $\frac{1-L}{L}$ and $d(L)$ for $g_1(L) = \frac{L^3}{0.2^3+L^3}$ and $g_2(L) = \frac{L^3}{0.6^3+L^3}$. For g_1 only certain values of L are steady states for some $d > 0$ as shown in Figure 11(b)-(d), whereas Figures 12(b) and (c) show that for g_2, every $0 < L < 1$ with $L \neq \frac{1}{2}$ is a steady state for some positive d. Comparing g_1 and g_2 we notice that the parameter in the denominator determines which case will occur.

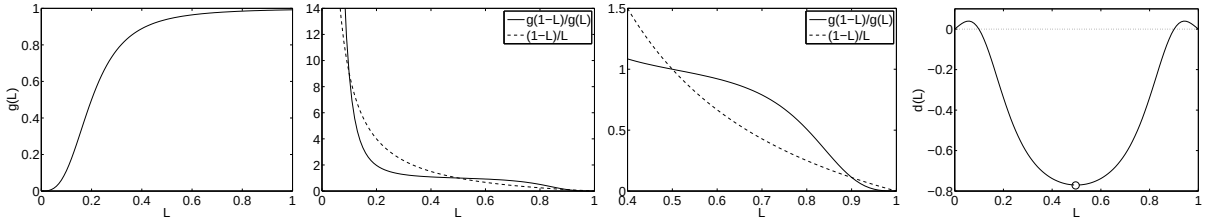

(a) (b) (c) (d)

Figure 11: Illustration of the existence of polarised steady states of system (6) for $g_1(L) = \frac{L^3}{0.2^3+L^3}$; only values of L close to 0 and close to 1 are polarised steady states; (a) plot of g_1, (b) plot of $\frac{g_1(1-L)}{g_1(L)}$ and $\frac{1-L}{L}$ (larger scale), (c) plot of $\frac{g_1(1-L)}{g_1(L)}$ and $\frac{1-L}{L}$ (zoomed in), (d) plot of $d(L)$, showing that it is only positive for values of L close to 0 and close to 1; the circle at $L = 0.5$ indicates the singularity.

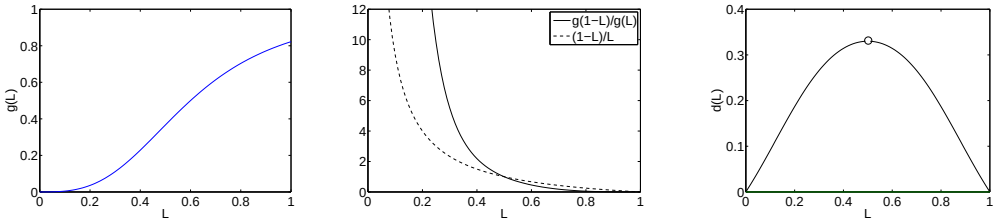

(a) (b) (c)

Figure 12: Illustration of the existence of polarised steady states of system (6) for $g_2(L) = \frac{L^3}{0.6^3+L^3}$. All $0 < L < 1$ with $L \neq \frac{1}{2}$ are polarised steady states; (a) Plot of $g_2(L)$, (b) Plot of $\frac{g_2(1-L)}{g_2(L)}$ and $\frac{1-L}{L}$. The two curves intersect only once, hence, conditions (9) and (10) are fulfilled and the polarised steady state exists always. (c) Plot of $d(L)$, it is positive for all L which we consider. The circle at $L = 0.5$ indicates the singularity.

Unpolarised period two patterns cannot arise because the initial amount of activity is the same in each cell and is conserved within a cell. In Section 3.2 we show that polarised period two patterns do not exist either.

3.2 Stability analysis

Linearising (7) about a steady state L and assuming $L_j = L + \tilde{l}_j$ yields

$$\begin{aligned}\dot{\tilde{l}}_j &= g(L+\tilde{l}_{j+1})(1-L-\tilde{l}_j) - g(1-L-\tilde{l}_{j-1})(L+\tilde{l}_j) + d(1-2L-2\tilde{l}_j)\\ &\approx -g(L)\tilde{l}_j + g'(L)\tilde{l}_{j+1}(1-L) - g(1-L)\tilde{l}_j + g'(1-L)\tilde{l}_{j-1}L - 2d\tilde{l}_j.\end{aligned}$$

Suppose $\tilde{l_j} = L_0 e^{ikj+\lambda t}$; dividing by $e^{ikj+\lambda t}$ we get

$$\lambda L_0 = (-g(L) + g'(L)e^{ik}(1-L) - g(1-L) + g'(1-L)e^{-ik}L - 2d)L_0, \tag{11}$$

which yields the dispersion relation $\lambda(k) = -g(L) + g'(L)e^{ik}(1-L) - g(1-L) + g'(1-L)e^{-ik}L - 2d$. Figure 13 shows $\lambda(k)$ for the homogeneous unpolarised steady state with $g(x) = \frac{2x^5}{0.6^5+x^5}$ and different values of d.

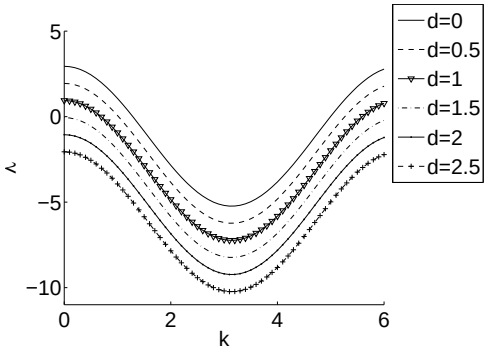

Figure 13: Dispersion relation of the homogeneous unpolarised steady state ($L = 0.5$) of (7) for $g = \frac{2x^5}{0.6^5+x^5}$ and different values of d. For $d \leq 0.5$ the system is unstable to homogeneous perturbations for certain k, and the system polarises. For $d \geq 1.5$ the system is stable to homogeneous perturbations, so all cells remain unpolarised.

Because of (11) the homogeneous unpolarised steady state $L = \frac{1}{2}$ is stable if $-g(\frac{1}{2}) + \frac{1}{2}g'(\frac{1}{2})\cos k < d$ for all k, i.e., if

$$-g\left(\frac{1}{2}\right) + \frac{1}{2}g'\left(\frac{1}{2}\right) < d, \tag{12}$$

since $g'(x) > 0$ for all x. Setting $h(L) := g(L)(1-L) - g(1-L)L + d(1-2L)$, the right hand side of (7) at a homogeneous steady state, (12) can be written as $h'(\frac{1}{2}) < 0$. The homogeneous polarised steady state $L \neq \frac{1}{2}$ is stable if

$$\frac{-g(L) + g'(L)\cos k(1-L) - g(1-L) + g'(1-L)L\cos k}{2} < d \qquad \text{for all } k, \tag{13}$$

since g is real. The left hand side of (13) is maximal for $\cos k = 1$. Thus, if (13) holds for $k = 0$ it holds for any k. This stability condition can be written as $h'(L) < 0$. Thus, the system cannot be simultaneously stable to homogeneous perturbations and unstable to inhomogeneous perturbations. Furthermore, the fastest growing mode is $k = 0$. Therefore, even polarised period two patterns, for which the total amount of activity in each cell would be conserved, cannot arise.

In summary, defining $h(L) := g(L)(1-L) - g(1-L)L + d(1-2L)$ yields $h(0) \geq 0$, $h(1) \leq 0$, $h(0) = -h(1)$, $h(\frac{1}{2}) = 0$ and $h'(0) = h'(1)$. Hence, the graph of h is rotationally symmetric about $(\frac{1}{2}, 0)$. The stability analysis reveals that a homogeneous steady state L is stable if $h'(L) < 0$. Depending on the forms of the function f and on the value of d, the function h has different forms, as

illustrated in Figure 14. In Figure 14(a) there is a stable pair of homogeneous polarised steady states and the homogeneous unpolarised steady state is unstable. Figure 14(b) and (c) show two cases in which only the homogeneous unpolarised steady state exists and is stable. We call these first three cases monostable. The last case, in Figure 14(d), we refer to as a bistable case because a pair of homogeneous polarised steady states as well as the homogeneous unpolarised steady state are stable. Furthermore, there exists a second pair of homogeneous polarised steady states, which are unstable.

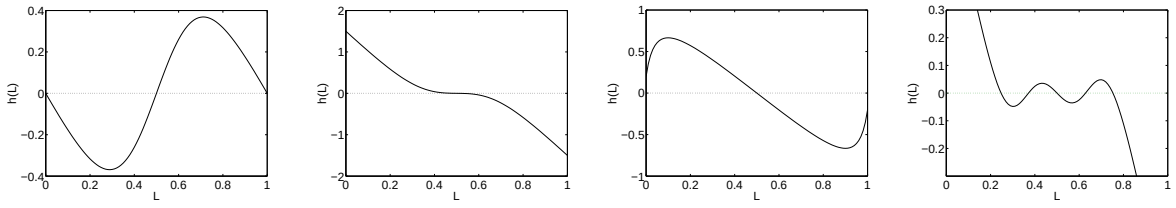

(a) (b) (c) (d)

Figure 14: Graphs of $h(L)$ for different forms of g and vallues of d. (a) Monostable case, $g(x) = \frac{2x^5}{0.6^5+x^5}$ and $d = 0$; (b) monostable case, $g(x) = \frac{2x^5}{0.6^5+x^5}$ and $d = 1.5$; (c) monostable case, $g(x) = \frac{x}{0.05+x}$ and $d = 0.2$; (d) bistable case, $g(x) = \frac{2x^6}{0.4^6+x^6}$ and $d = 0.8$.

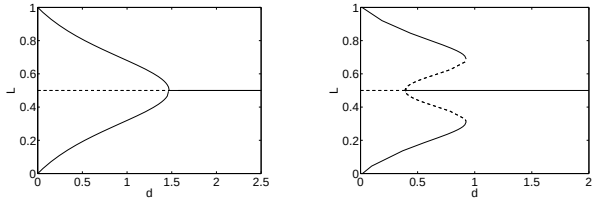

(a) (b)

Figure 15: Bifurcation diagrams for (a) $g(x) = \frac{2x^5}{0.6^5+x^5}$ and (b) $g(x) = \frac{2x^6}{0.4^6+x^6}$; increasing d above a threshold disrupts polarity.

Figure 15 shows the bifurcation diagrams for $g(x) = \frac{2x^5}{0.6^5+x^5}$ and $g(x) = \frac{2x^6}{0.4^6+x^6}$. The diagram for our third choice of g was omitted because in this case the homogeneous unpolarised steady state is the only stable steady state for any d. In the two cases in Figure 15, increasing the diffusion parameter d above a certain threshold, depending on g, disrupts polarity and results in only the homogeneous unpolarised steady state being stable. However, for values of d below these thresholds the behaviour of the system depends on the function g. In the first case, depicted in Figure 15(a), the polarity gets weaker if we increase d from zero until the two branches for the two homogeneous polarised steady states merge with the branch for the homogeneous unpolarised steady state. On the contrary, in the second case the branches for polarised steady states do not merge but the states disappear in a pair of saddle-node bifurcations if d is increased above about 0.9.

3.3 Travelling wave solutions

If $g'(\frac{1}{2}) > 2\,(g(\frac{1}{2}) + d)$, system (7) has an unstable unpolarised steady state $L = \frac{1}{2}$ and a stable polarised steady state $L^* > \frac{1}{2}$. Thus, we expect waves taking $L_j = \frac{1}{2}$ to $L_j = L^*$ similar to the travelling wave solutions of Fisher's equation [9], but in a discrete system like the ones studied by Elmer and Van Vleck [5], Keener [6] and Owen [10]. Introduction of the travelling wave coordinate $s = j - ct$ with $L_j(t) = f(j - ct) = f(s)$ yields

$$-c\frac{\mathrm{d}\,f}{\mathrm{d}\,s} = g(f(s+1))(1 - f(s)) - g(1 - f(s-1))f(s) + d(1 - 2f(s))$$

with

$$0 \leq f \leq 1, \lim_{s\to-\infty} f(s) = L^* \text{ and } \lim_{s\to+\infty} = \frac{1}{2}.$$

Linearising about a steady state F with $f(s) = F + \tilde{f}(s)$, we get

$$-c\dot{\tilde{f}}(s) \approx -g(F)\tilde{f}(s) + g'(F)\tilde{f}(s+1)(1-F) - g(1-F)\tilde{f}(s) + g'(1-F)\tilde{f}(s-1)F - 2d\tilde{f}(s).$$

Assuming $\tilde{f}(s) = F_0 e^{\lambda s}$ and dividing by $F_0 e^{\lambda s}$ yields

$$-c\lambda = -g(F) - g(1-F) + g'(F)e^{\lambda}(1-F) + g'(1-F)e^{-\lambda}F - 2d. \tag{14}$$

Provided the initial amount $L_j(0) \in [\frac{1}{2}, L^*)$, the activity on the left side of the cell will never decrease below $\frac{1}{2}$. We will show this by contradiction. Let $L_j(0) \geq \frac{1}{2}$ for all j and assume $j = k$ is the first point at which L_j crosses through $\frac{1}{2}$ at time $t = t^*$. Hence, we would have $L_k(t^*) = \frac{1}{2}, L_{k+1}(t^*) \geq \frac{1}{2}$, $L_{k-1}(t^*) \geq \frac{1}{2}$ and $\dot{L}_k(t^*) \leq 0$. However, substituting $L_k = \frac{1}{2}$ into (7) yields

$$\dot{L}_k = \frac{1}{2}(g(L_{k+1}) - g(1 - L_{k-1})) \geq 0,$$

with equality only if $L_{k+1} = L_{k-1} = \frac{1}{2}$, since g is increasing. This is a contradiction; thus, there are no spatially oscillatory solutions of system (7) given the above initial conditions. Thus, the wave speed c is determined by the condition that there have to be real roots of equation (14). Assuming $F = \frac{1}{2}$, i.e., looking ahead of the wave, (14) yields

$$-c\lambda = -2\left(g\left(\frac{1}{2}\right) + d\right) + g'\left(\frac{1}{2}\right)\cosh(\lambda), \tag{15}$$

with the two cases

$$-2\left(g\left(\frac{1}{2}\right) + d\right) + g'\left(\frac{1}{2}\right) < 0 \ (L = \tfrac{1}{2} \text{ is stable}): \text{ two real roots for all } c,$$
$$-2\left(g\left(\frac{1}{2}\right) + d\right) + g'\left(\frac{1}{2}\right) > 0 \ (L = \tfrac{1}{2} \text{ is unstable}): \text{ real roots only if } c \geq c_{min}.$$

Figure 16 shows the plots of the two sides of (15) for $g(x) = \frac{2x^5}{0.6^5+x^5}$ and $d = 1.9$ as an example of the first case and for the same g and $d = 0$ as an example of the second case (see also Figure 15(a)). We can see that the right hand side of (15) is minimal at zero. In the first case in Figure 16(a) the value at this minimum is less than zero, whereas in the second case it is greater than zero (see Figure 16(b)). Since all graphs for the left hand side of (15) go through the origin we get two real roots for all c in Figure 16(a) and only real roots for c above a certain minimum value in Figure 16(b). For our choice of g and d this minimum value lies between 5 and 6.

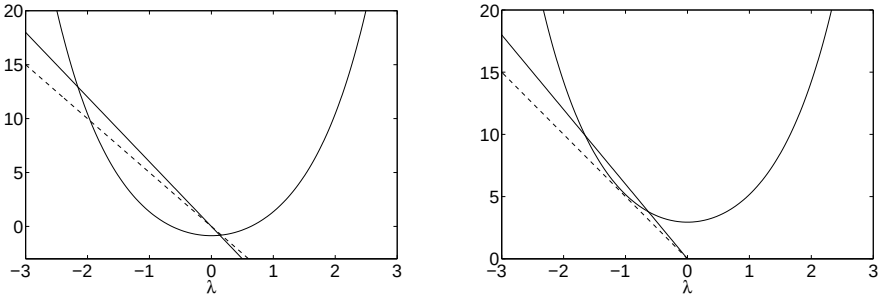

(a) (b)

Figure 16: Graphs of the two sides of equation (15) for $g(x) = \frac{2x^5}{0.6^5+x^5}$ and different d to determine the possible wave speeds c of the travelling wave solution of system (7) (solid line $c = 6$, dashed line $c = 5$); (a) $d = 1.9$, there are two real roots for all c, i.e. any c is a wave speed; (b) $d = 0$, we only get real roots if $c \geq c_{min}$, i.e. a minimum wave speed c_{min} exists, in this case $5 < c_{min} < 6$.

As a next step we assume that initially we have a single polarised cell (L_p, R_p) in the middle of a row of unpolarised cells. For suitable choices of g and d, a polarising wave is initiated by cell p and spreads out in both directions into the unpolarised regions. We want to analyse the speed of this wave. To simplify matters we assume $d = 0$ and (L_p, R_p) either $(L^*, 0)$ or $(0, L^*)$ for $L^* > \frac{1}{2}$. Let $L_p = L^*$ in the initial conditions.

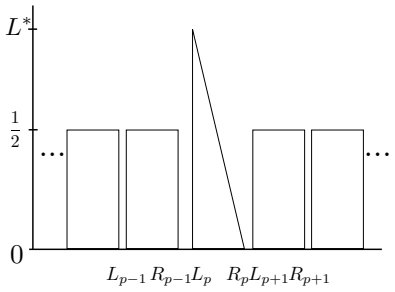

Figure 17: Initial conditions, which we assume to show that the speed of a travelling wave solution of system (7) may depend on its direction.

By substituting in (7) we get

$$\dot{L}_{p+1} = \frac{1}{2}\left(g\left(\frac{1}{2}\right) - g(1-L^*)\right) \geq 0,$$
$$\dot{L}_{p-1} = \frac{1}{2}\left(g(L^*) - g\left(\frac{1}{2}\right)\right) \geq 0,$$

since g is increasing. Therefore, if $g(\frac{1}{2}) - g(0) < g(L^*) - g(\frac{1}{2})$, the wave initially moves faster to the left (decreasing indices). By symmetry we conclude if $L_p < \frac{1}{2}$ initially and $g(\frac{1}{2}) - g(0) < g(L^*) - g(\frac{1}{2})$, the early wave moves faster to the right (increasing indices). This analysis suggests that the speed of the wave may depend on its direction.

3.4 Numerical Simulations

We simulated the model (6) for a row of 100 cells using the Matlab ODE solver ode45. The boundary conditions were $l_0 = l_1$ and $l_{101} = l_{100}$, which are compatible with the boundary conditions we chose for the analysis of the homogeneous steady states. Moreover, we will see in Figure 19 that the boundary conditions do not have an effect on the travelling wave solution as soon as the wave front has moved away from the boundary. Figures 18 and 19 show the final states for two different initial conditions. In Figure 18(a) there is an imbalance in each cell for the whole row. The simulations were performed using $g(x) = \frac{2x^5}{0.6^5+x^5}$, a function for which we analysed the properties of system (6) in Section 3.2. Consistent with our analysis we get the completely polarised steady state for $d = 0$ (see Figure 18(b)), which gets weaker as we increase d (see Figure 18(c)) and disappears once d is greater than a certain threshold (see Figure 18(d)). These results match the corresponding bifurcation diagram in Figure 15(a). The direction of polarisation of the homogeneous polarised steady state depends only on the direction of the initial conditions. For $g(x) = \frac{2x^6}{0.4^6+x^6}$ and $d = 0.5$, a bistable case (see Figure 15(b)), we need sufficiently strongly polarised initial conditions to get polarisation, otherwise the homogeneous unpolarised steady state occurs (result not shown). This is not surprising as we know from the analysis that both states are stable for this choice of g and d.

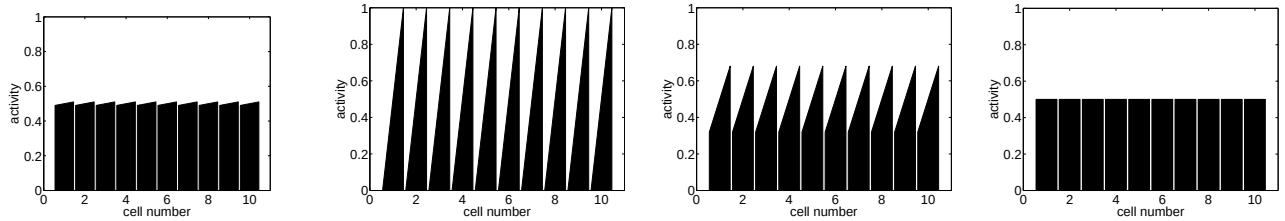

Figure 18: Final states for system (6) with $g(x) = \frac{2x^5}{0.6^5+x^5}$ and different values of d; (a) initial condition, $L_j = 0.49$ for all j; (b) result for $d = 0$, strong polarity; (c) result for $d = 1$, weaker polarity; (d) result for $d = 1.9$, unpolarised steady state.

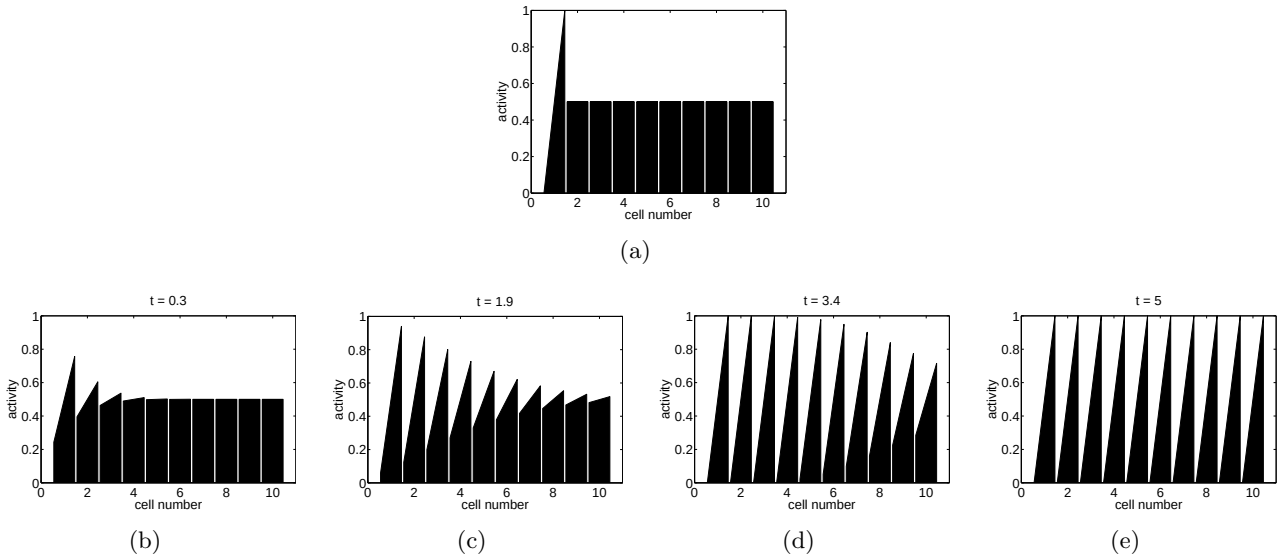

(a) (b) (c) (d) (e)

Figure 19: Wave propagation. (a) Initial condition; (b)–(e) the state of system (6) at different points in time for $g(x) = \frac{2x^5}{0.6^5+x^5}$ and $d = 0$.

With the initial condition depicted in Figure 19(a) only the first cell of the row is polarised while the rest remain unpolarised. For small values of d this results in the propagation of a wave that propagates with a speed that depends on g. The wave for $g(x) = \frac{2x^5}{0.6^5+x^5}$ and $d = 0$ is shown in Figure 19. Weakening the polarity in the first cell of the initial condition does not change the result.
The analysis in Section 3.3 shows that, for our chosen $g(x) = \frac{2x^5}{0.6^5+x^5}$ and $d = 0$, there exists a minimum wave speed which is 5.15. The wave speed calculated from the simulations is 5.09, which matches the theoretical value reasonably well. A difference of the wave speed for different directions could not be detected. We have conducted the same calculations and simulations for other choices of g. The results are summarised in Table 1, which shows the theoretical value for the minimum wave speed and the numerical values for both directions of the wave.

	Wavespeed		
Function g, Diffusion d	**Theoretical minimum value**	**Numerical value First cell init. (0,1)**	**First cell init. (1,0)**
$g(x) = \frac{x^3}{0.6^3+x^3},\ d = 0$	1.4	1.4	1.4
$g(x) = \frac{3x^4}{0.7^4+x^4},\ d = 0$	4.83	4.8	4.8
$g(x) = \frac{2x^6}{0.4^6+x^6},\ d = 0$	2.52	2.4	5.2
$g(x) = \frac{4x^3}{0.5^3+x^3},\ d = 0.5$	3.51	3.4	4.3

Table 1: Theoretical and numerical results of wave speed calculations for different choices of g and d and different initial conditions.

The theoretical value of the minimum wave speed and the minimum of the numerical values of the wave speed agree well. In the first two cases the wave speed does not depend on the direction, whereas

in the third and fourth case we get a significant difference. For the two latter cases the wave is faster if the first cell in the initial conditions is polarised to the left, i.e., $(L_1, R_1) = (1, 0)$. This matches our analysis since for both g the inequality $g(0.5) - g(0) > g(1) - g(0.5)$ holds.

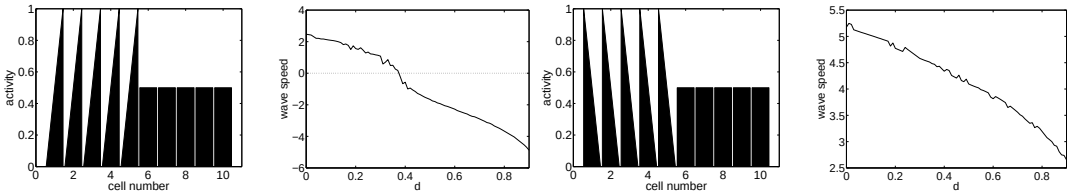

(a) (b) (c) (d)

Figure 20: Analysis of the travelling wave solution of system (6) for $g(x) = \frac{2x^6}{0.4^6+x^6}$. (a) Initial condition which gives wave reversal; (b) Graph of wave speed for initial condition in (a); (c) Initial condition which does not give propagation failure; (d) Graph of wave speed for initial condition (c).

We analysed the travelling wave solution for $g(x) = \frac{2x^6}{0.4^6+x^6}$ in more detail. In the corresponding bifurcation diagram (see Figure 15(b)) we can see that there is an interval $[d_1, d_2]$ for which system (6) is bistable. Starting with the initial condition shown in Figure 20(a) we found out that for $d < d_1$ the wave front moves to the right into the unpolarised region and for $d > d_1$ it moves to the left into the polarised region. Hence, we expect propagation failure at d_1. This is supported by the graph in Figure 20(b). We plotted the wave speed against the diffusion parameter d for system (6) with $g(x) = \frac{2x^6}{0.4^6+x^6}$. As we can see the wave speed is positive up to a d close to 0.4 and then becomes negative. If we choose the initial condition in Figure 20(c) we do not get propagation failure (see Figure 20(d)). We obtained similar results for other choices of g for which system (6) is bistable for some d.

Behaviour for irregularities in the initial conditions

To analyse the behaviour of the model when the initial conditions contain irregularities we distinguish between polarisation because of a global weak initial polarity as in Figure 18 and polarisation via a wave as in Figure 19. In the case of the global weak initial polarity we have introduced a couple of cells that are weakly polarised in the wrong direction (see Figure 21 (a)). We choose $g(x) = \frac{2x^5}{0.6^5+x^5}$, the function used to generate Figures 18 and 19. In Figure 21 we see that each cell in the row initiates a wave and the meeting of the wave fronts determines whether an irregularity is corrected. For our choice of parameter values and initial conditions we get correct polarity over the whole row.

To analyse the potential of the wave to overcome anomalies in the initial conditions we included one cell that points in the wrong direction (see Figure 22(a)). We chose $g(x) = \frac{2x^6}{1.5^6+x^6}$ and $d = 0$. Two waves are initiated and the one propagating polarity to the right finally overcomes the one initiated

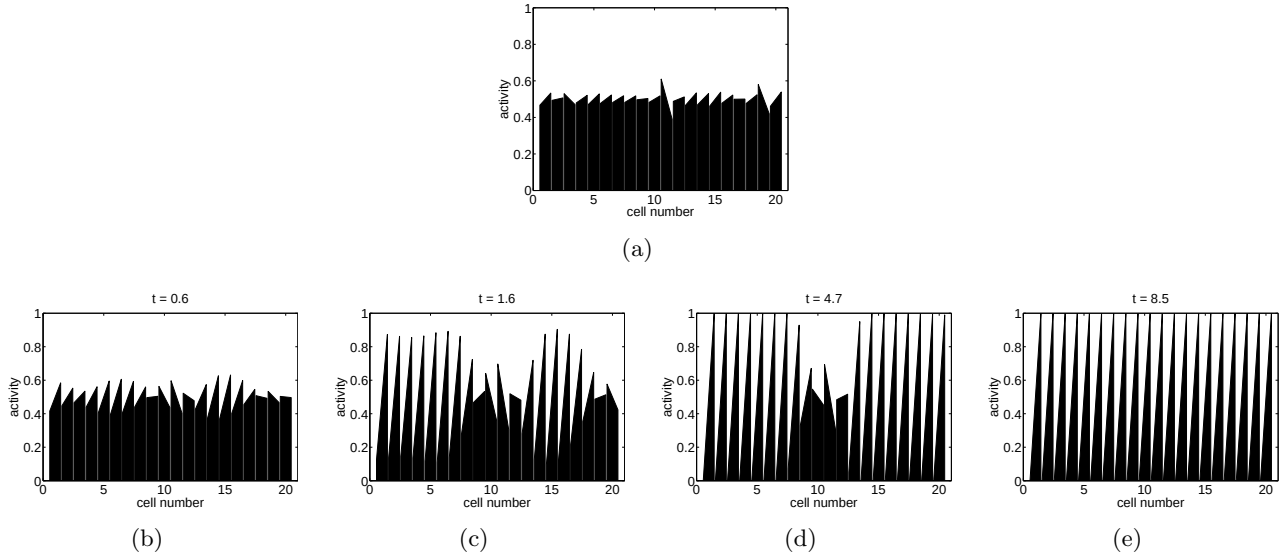

(a) (b) (c) (d) (e)

Figure 21: Irregularities in the global initial polarity. (a) Initial condition; (b)–(e) state of the system (6) at different points in time for $g(x) = \frac{2x^5}{0.6^5+x^5}$ and $d = 0$.

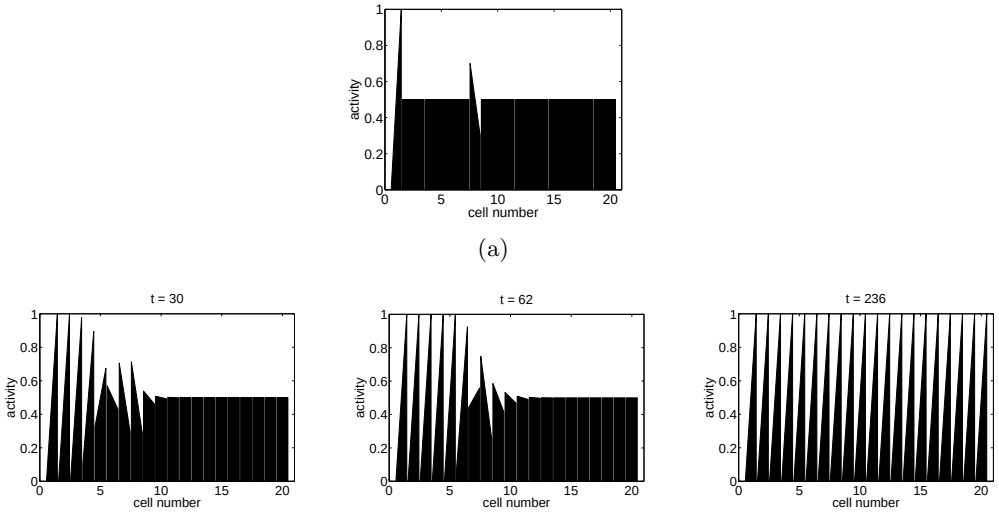

(a) (b) (c) (d)

Figure 22: Waves can correct single cells. (a) Initial condition–one cell is initially polarised in the wrong direction; (b)–(d) state of the system (6) at different points in time for $g(x) = \frac{2x^6}{1.5^6+x^6}$ and $d = 0$.

by the irregular cell. Hence, waves can overcome single cells that initially point the wrong way.
Most of the dynamics in a row of cells can be explained by the interactions of only two cells. These are summarised in the phase plane in Figure 23, for which we chose the same g and d as in Figure 22. There are four steady states (two stable and two unstable) indicated by crosses. Note that $(L_1, L_2) = (0, 1)$ is not a steady state. If we imagine the diagonal from $(0, 1)$ to $(1, 0)$, for every initial condition above this diagonal the system will tend to $(1, 1)$ and from anywhere below the diagonal it will tend to $(0, 0)$. For example, if we start at about $(0.35, 0.65)$, corresponding to cells 5 and 6 in Figure 22(b) the phase plane predicts these two cells will tend to the steady state $(L_5, L_6) = (0, 0)$. An example of this behaviour is shown in Figure 22(c).

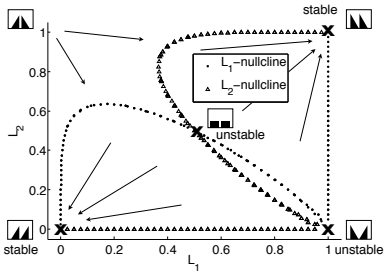

Figure 23: Phase plane for the two cell model with $g(x) = \frac{2x^6}{1.5^6+x^6}$ and $d = 0$. There are four steady states, indicated by crosses, two of which are stable. Initial conditions above the diagonal from (0,1) to (1,0) yield the steady state (1,1) and initial conditions below the diagonal give rise to (0,0).

The analysis reveals that whether or not a wrongly polarised cell can be corrected by a polarising wave depends on the initial distance between this anomaly and the wave front and the strength of the anomaly. In addition we have to take into account that the wave has a different speed depending on its direction. In Figure 22 the wave to the right initiated by cell 1 is faster than the wave in the same direction initiated by cell 8. Therefore it is possible to achieve correct polarity.

Analysis of clones

Similar to Section 2.3 we include clones in the row of cells and investigate their effects on the surrounding cells. Figure 24 shows the results for a clone in which the cells have less activity than the wild-type cells. As feedback function we have chosen $g(x) = \frac{2x^6}{0.4^6+x^6}$. The corresponding bifurcation diagram for this choice of g in Figure 15(b) shows that system (6) exhibits two bifurcations at $d_1 \approx 0.4$ and $d_2 \approx 0.9$. The initial conditions are shown in the first column of Figure 24.

The difference between the two initial conditions is the strength of the initial global cue in the surrounding wild-type cells. Columns two to four display the resulting final states for different values of d. At both boundaries of the clone a patterning wave is initiated which propagates away from the

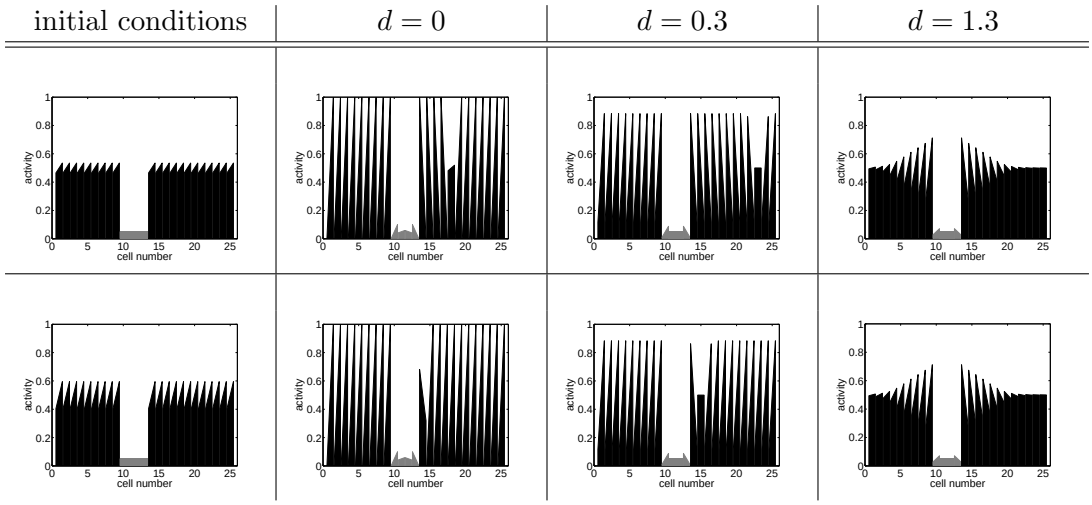

Figure 24: Final states of system (6) for a clone with low activity (shown in grey) and a weak initial polarisation in the surrounding cells. In the first row the difference between left and right side is initially 0.07; in the second row 0.19. Simulations performed using $g = \frac{2x^6}{0.4^6+x^6}$ and different values of d.

clone.

Domineering nonautonomy occurs in the direction of the initial global cue. As can be seen in Figure 24, its range depends both on the strength of the global cue in the surrounding cells and on the diffusion parameter. Increasing d up to d_2 increases the range of the effect of the clone. If $d > d_2$, the wave initiated at the clone boundaries spreads only a few cells into the surrounding region. The rest of the wild-type cells are unpolarised. This is due to the fact that for this choice of g and d the polarised state is no longer a steady state of system (6). In this case, the unpolarised state is the only stable steady state (see also Figure 15(b)). Simulations using $g(x) = \frac{2x^5}{0.6^5+x^5}$ gave similar results.

As a next step, we set the activity in the clone to be higher than in the surrounding cells. If we choose $g(x) = \frac{2x^5}{0.6^5+x^5}$ (see Figure 15(a) for corresponding bifurcation diagram), the disrupting effect of the clone spreads in the direction opposite to the direction of the initial global cue in the wild-type cells (see Figure 25(b)). As above, a weaker initial global cue yields a wider range of domineering nonautonomy. Furthermore, increasing d up to the bifurcation point d_3 increases the range of the effect of the clone. For $d > d_3$, the wave initiated by the clone spreads only three cells into the surrounding region. The rest of the wild-type cells are unpolarised. This is because the unpolarised state is the only stable steady state of system (6) for this choice of parameter values.

For $g(x) = \frac{2x^6}{0.4^6+x^6}$, the clone does not affect polarity in surrounding cells for small d as shown in Figure 25(c). This is due to the difference in wave speed in different directions for this function (see Table 1). Any possible disruptions get corrected by a fast wave coming from the opposite side of the clone and moving through the clone. For $d = 0.5$, which is greater than d_1, the unpolarised steady

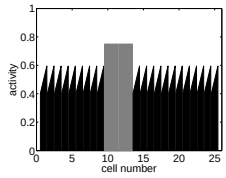

(a)

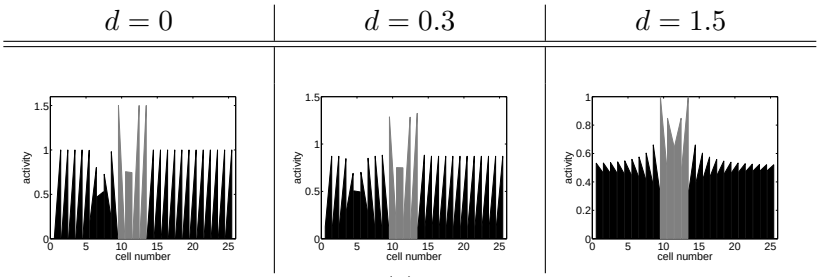

(b)

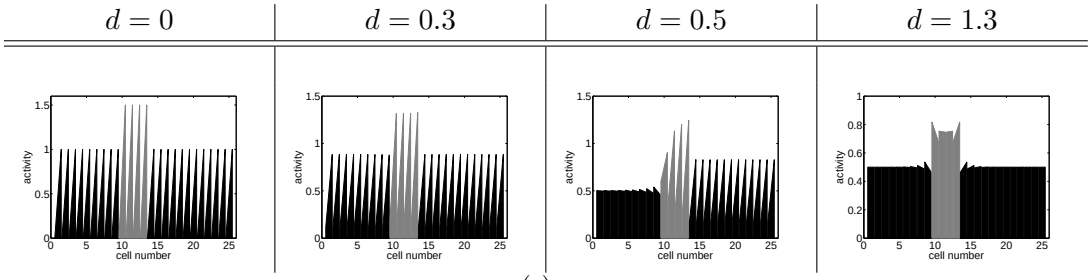

(c)

Figure 25: Final states of system (6) for a clone with high activity (shown in grey) and a weak initial polarisation in the surrounding cells. (a) Initial condition in which the difference between left and right side in the wild-type cells is 0.19. (b) Final states for $g(x) = \frac{2x^5}{0.6^5+x^5}$ and different values of d. (c) Final states for $g(x) = \frac{2x^6}{0.4^6+x^6}$ and different values of d.

state spreads as a wave from the clone in the direction opposite to the direction of the initial global cue. If we decrease the strength of the initial global cue in the wild-type cells, the polarisation of the cells on the other side of the clone fails as well and we get a result similar to the one for $d = 1.3$, which shows propagation failure on both sides of the clone.

Assigning a different feedback strength to cells in the clone to that in the surrounding cells only yields an effect if for the chosen diffusion parameter d the stability of system (6) is different for the two g. Let $g_1(x) = \frac{2x^6}{0.4^6+x^6}$ represent the feedback function in the wild-type cells and $g_2(x) = \frac{2x^5}{0.6^5+x^5}$ the feedback in the clone. The clone only affects surrounding cells if $d_1 < d < d_3$. If $d = 0.5$, the polarised state is the only stable steady state of system (6) for g_2 and for g_1 system (6) is bistable (see Figure 15). In this case a polarising wave is initiated in the clone and from there it spreads in the direction opposite to the direction of the initial global cue (first row of Figure 26). Increasing the initial global cue sufficiently will yield polarisation of the whole row because then for the chosen g_1 system (6) tends

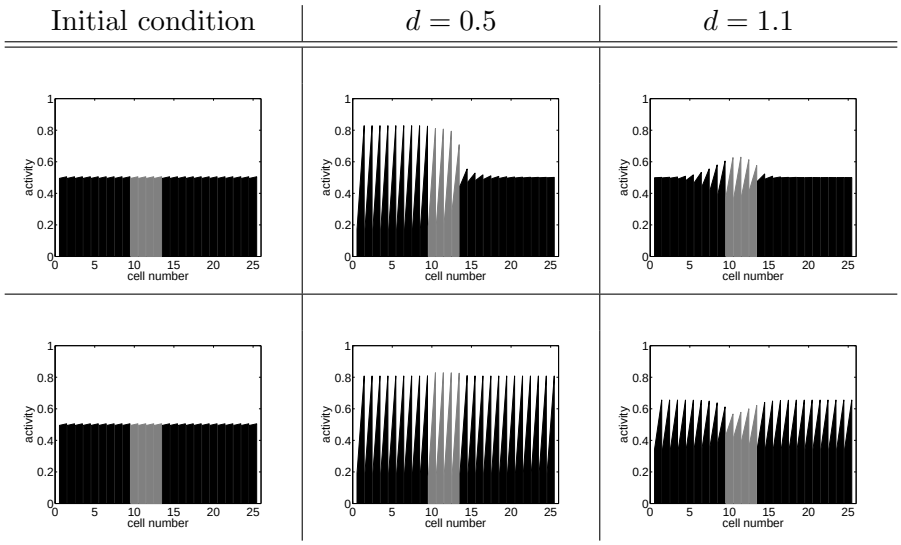

Figure 26: Effects of a clone of cells with different strength of feedback than that in the surrounding cells. First row: feedback in the wild-type cells is represented by $g_1(x) = \frac{2x^6}{0.4^6+x^6}$, feedback in the clone by $g_2(x) = \frac{2x^5}{0.6^5+x^5}$; second row: g_2 represents the feedback in the wild-type cells and g_1 the feedback in the clone.

to the polarised steady state. If $d = 1.1$, for g_1 system (6) is monostable and the stable steady state is $L_j = \frac{1}{2}$ for all j; for g_2 the polarised steady state is still stable. We get a polarising wave initiated in the clone, that only spreads a couple of cells into the surrounding cells. It spreads a little further in the direction opposite to the direction of the initial global cue (see Figure 26, first row, last column). If we choose g_1 as the feedback function in the clone and g_2 for the feedback in the surrounding cells we get the polarised steady state in the whole row for $d = 0.5$. There is, however, a slight difference in the amount of activity between the clone and the surrounding cells, in that the peaks in the clone are slightly higher (see Figure 26, second row, second column). For $d = 1.1$ a polarising wave spreads from both ends into the clone. Whether or not this wave can polarise the clone completely depends on the size of the clone, as shown in Figure 27. In Figure 27(b) the wave from the right side spreads further into the clone than from the left side because for our choice of g the wave is faster in that direction. Changing the strength of the initial global cue does not alter how far the waves spread into the clone (not shown).

4 Discussion

Based on the general consensus that the conserved second tier of PCP generation depends on a feedback loop that amplifies an initial global cue, we have developed models based on two generic feedback mechanisms that can generate polarity. To maximise the mathematical tractability of the models, we have used simple systems of equations that encompass a wide range of more specific mechanistic

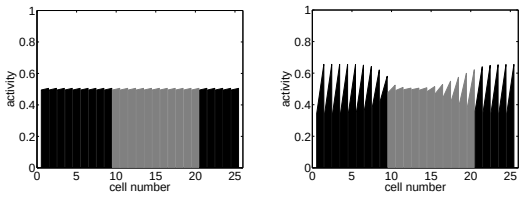

(a) (b)

Figure 27: The effect of a large clone of cells with different strength of feedback to that in the surrounding cells; $g_2(x) = \frac{2x^5}{0.6^5+x^5}$ represents the feedback in the wild-type cells and $g_1(x) = \frac{2x^6}{0.4^6+x^6}$ the feedback in the clone. (a) Initial condition; (b) Final state for system (6) for $d = 1.1$.

models. We have employed a combination of linear stability analysis and numerical simulations to investigate the patterns of cell polarity that each model can generate.

The feedback and diffusion model can generate both period two and polarised patterns. To achieve polarisation, the intercellular feedback has to be sufficiently strong and the intracellular diffusion sufficiently weak. Moreover, uniform initial conditions are needed. We have also shown that the model can overcome small anomalies in the initial conditions. Analysis of clones of cells that have a different amount of activity than the surrounding cells revealed that the range of the effect of these clones depends on both the strength of the initial global cue in the surrounding wild-type cells and on the value of diffusion parameter. These results also hold for clones in which the strength of the feedback is different to that in the surrounding cells. The feedback and diffusion model is not conservative — the PCP activity in a cell can be time-varying. However, if the activity in this model is interpreted as representing non-conserved protein complexes, the overall amounts of the proteins that combine to form complexes could be conserved in each cell. Furthermore, this type of conservative model can be derived by elimination of variables in a conservative model. As an example of this, assume that a cell is divided into three parts: a left, a right and a central compartment. Representing the activity in each compartment in cell j by l_j, r_j and c_j, respectively, a model corresponding to the system can be written as:

$$\begin{aligned}
\dot{l}_j &= -l_j + f(r_{j-1}) + d(r_j - l_j),\\
\dot{r}_j &= -r_j + f(l_{j+1}) + d(l_j - r_j),\\
\dot{c}_j &= l_j + r_j - f(r_{j-1}) - f(l_{j+1}),
\end{aligned}$$

for which $\dot{u_j} + \dot{l_j} + \dot{r_j} = 0$. Thus, although the model as a whole is conservative, the activities on the left and right sides of a cell may not be conserved (if the central compartment is not considered in the model).

As an alternative approach, we have proposed a conservative model that can generate polarisation of a row of cells either as a result of a global weak initial polarisation of every cell or via a travelling

wave emanating from a single cell or boundary. Both can be reasonable ways of spreading polarity over a whole region of cells. In addition to investigating the stability of steady states in this model, we also explored the factors that determine the behaviour of the travelling wave. We found that in some cases the speed of the wave depends on its direction of travel. Furthermore, for certain feedback functions and diffusion coefficients, wave reversal could be detected. We demonstrated that this model has the potential to correct irregularities in the initial conditions for both a global initial polarity cue and under conditions that result in a travelling wave. We also analysed the effects of clones on the surrounding cells. For clones of cells having a different amount of PCP activity than that in surrounding cells, the strength of the initial global cue in the wild-type cells and the strength of the intracellular diffusion influenced the range of the effect of the clone. Especially for the clones with different strength of feedback compared to the surrounding cells, the effect of the clone was dependent on the stability behaviour of the model for the chosen parameters.

We have restricted our analysis of the two models to one spatial dimension. However, both can be extended to fields of square or hexagonal cells. Taking the feedback and diffusion model as an example, we can formulate the system of equations for a field of square cells as illustrated in Figure 28 as

$$\begin{aligned}
\dot{l}_{i,j} &= -l_{i,j} + f(r_{i,j-1}) + d(a_{i,j} + b_{i,j} - 2l_{i,j}),\\
\dot{r}_{i,j} &= -r_{i,j} + f(l_{i,j+1}) + d(a_{i,j} + b_{i,j} - 2r_{i,j}),\\
\dot{a}_{i,j} &= -a_{i,j} + f(b_{i-1,j}) + d(l_{i,j} + r_{i,j} - 2a_{i,j}),\\
\dot{b}_{i,j} &= -b_{i,j} + f(a_{i+1,j}) + d(l_{i,j} + r_{i,j} - 2b_{i,j}),
\end{aligned} \tag{16}$$

where f is a decreasing positive function, with $f(0)$ finite and positive and $d \geq 0$. In addition, the analysis of the models can be extended to spatially-graded initial conditions. Since there is to date no specific experimental evidence supporting a particular form for the polarity cues generated by the first tier of the PCP mechanism, a weak initial polarity in each cell and an initial gradient are both potentially reasonable forms of initial cues.

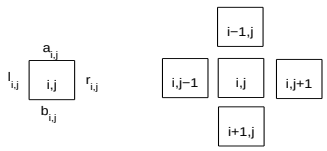

Figure 28: Labelling of cells in a two-dimensional model (16).

In contrast to the existing models by Le Garrec *et al.* [8] and Amonlirdviman *et al.* [2], the models

that we study here are not based on detailed assumptions about interactions of specific PCP core proteins. Rather, they encode a more general picture of possible mechanisms driving the second tier of the PCP mechanism. This approach raises several questions. In both our models, the strength of intracellular diffusion is a key component, which affects the behaviour of the models. It would be interesting to investigate experimentally whether changing intracellular movement affects the overall pattern of planar polarity in a system such as the *Drosophila* wing. Furthermore, we refer to the variables in our models as amounts of "activity", leaving open the question of what they represent in terms of specific molecular species. A concrete assignment of molecular identity to the activities in our models depends on the answer to a key question: what is it that polarises cells? In wild-type tissue of the *Drosophila* larval wing, the core PCP proteins become distributed asymmetrically in the membrane of cells shortly before the hairs start to grow. However, recently reported experiments show that *Drosophila* larval wings that are mutant for certain core proteins do not display asymmetric distribution of the core proteins, but nonetheless show normal hair development [15]. These results suggest that mechanisms other than asymmetric localisation of the core PCP proteins may be polarising the cells, such as asymmetric distribution of certain protein complexes or other intracellular components. Comparing experimental findings with the different behaviour of our models under different parameter combinations will also provide an opportunity to rule out parameter sets and give a better idea of the underlying feedback mechanism.

Acknowledgement

This work was supported by grant no. EP/C539044/1 and EP/C539052/1 from the Engineering and Physical Sciences Research Council.

References

[1] P. N. Adler, 2002, Planar signaling and morphogenesis in *Drosophila.*, Dev. Cell, 2, 525–535.

[2] K. Amonlirdviman, N. A. Khare, D. R. P. Tree, W.-S. Chen, J. D. Axelrod, and C. J. Tomlin, 2005, Mathematical modeling of planar cell polarity to understand domineering nonautonomy., Science, 307, 423–426.

[3] W.-S. Chen, D. Antic, M. Matis, C. Y. Logan, M. Povelones, G. A. Abderson, R. Nusse, and J. D. Axelrod, 2008, Asymmetric homotypic interactions of the atypical cadherin flamingo mediate intercellular polarity signaling, Cell, 133, 1093–1105.

[4] J. R. Collier, N. A. M. Monk, P. K. Maini, and J. H. Lewis, 1996, Pattern formation by lateral inhibition with feedback: A mathematical model of Delta-Notch intercellular signalling., J. Theor. Biol., 183, 429–446.

[5] C. E. Elmer and E. S. Van Vleck, 1999, Analysis and computation of travelling wave solutions of bistable differential-difference equations, Nonlinearity, 12, 771–798.

[6] J. P. Keener, 1987, Propagation and its failure in coupled systems of discrete excitable cells, SIAM J. Appl. Math., 47, 556–572.

[7] J.-F. Le Garrec and M. Kerszberg, 2008, Modeling polarity buildup and cell fate decision in the fly eye: insight into the connection between the PCP and Notch pathways, Dev. Genes Evol., 218, 413–426.

[8] J.-F. Le Garrec, P. Lopez, and M. Kerszberg, 2006, Establishment and maintenance of planar epithelial cell polarity by assymetric cadherin bridges: A computer model., Dev. Dyn., 235, 235–246.

[9] J. D. Murray, 1989, Mathematical Biology. Springer-Verlag.

[10] M. R. Owen, 2002, Waves and propagation failure in discrete space models with nonlinear coupling and feedback, Physica D, 173, 59–76.

[11] E. Plahte and L. Øyehaug, 2007, Pattern-generating travelling waves in a discrete multicellular system with lateral inhibition, Physica D, 226, 117–128.

[12] R. L. Raffard, K. Amonlirdviman, J. D. Axelrod, and C. J. Tomlin, 2008, An adjoint-based parameter identification algorithm applied to planar cell polarity signaling, IEEE Trans. Autom. Control, 53 (Special Issue on Systems Biology), 109–121 [DOI: 10.1109/TAC.2007.911362].

[13] M. Simons and M. Mlodzik, 2008, Planar cell polarity signaling: From fly development to human disease, Ann. Rev. Genetics.

[14] D. Strutt, 2002, The asymmetric subcellular localisation of components of the planar polarity pathway, Sem. Cell Dev. Biol., 13, 225–231.

[15] D. Strutt and H. Strutt, 2007, Differential activities of the core planar polarity proteins during *Drosophila* wing patterning, Dev. Biol., 302, 181–194.

[16] C. R. Vinson and P. N. Adler, 1987, Directional non-cell autonomy and the transmission of polarity information by the frizzled gene of *Drosophila*, Nature, 329, 549–551.

[17] J. Wu and M. Mlodzik, 2008, The frizzled extracellular domain is a ligand for Van Gogh/Stbm during nonautonomous planar cell polarity signaling, Dev. Cell, 15, 462–469.

[18] T. Xu and G. M. Rubin, 1993, Analysis of genetic mosaics in developing and adult *Drosophila* tissues, Development, 117, 1223–1237.